Journal of Solid State Chemistry 191 (2012) 153–157

Contents lists available at SciVerse ScienceDirect

Journal of Solid State Chemistry

journal homepage: www.elsevier.com/locate/jssc

$K_2NaOsO_{5.5}$ and $K_3NaOs_2O_9$: The first osmium perovskites containing alkali cations at the "*A*" site

Kailash M. Mogare [1], Wilhelm Klein [2], Martin Jansen *

Stuttgart, Max-Planck-Institut für Festkörperforschung, Heisenbergstraße 1, 70569 Stuttgart, Germany

ARTICLE INFO

Article history:
Received 19 October 2011
Received in revised form
7 March 2012
Accepted 12 March 2012
Available online 18 March 2012

Keywords:
Osmium
Double Perovskite
Triple Perovskite
High oxygen pressure synthesis

ABSTRACT

$K_2NaOsO_{5.5}$ and $K_3NaOs_2O_9$ were obtained from solid-state reactions of potassium superoxide, sodium peroxide and osmium metal at elevated oxygen pressures. $K_2NaOsO_{5.5}$ crystallizes as an oxygen-deficient cubic double perovskite in space group $Fm\overline{3}m$ with $a=8.4184(5)$ Å and contains isolated OsO_6 octahedra. $K_3NaOs_2O_9$ crystallizes hexagonally in $P6_3/mmc$ with $a=5.9998(4)$ Å and $c=14.3053(14)$ Å. $K_3NaOs_2O_9$ consists of face sharing Os_2O_9 pairs of octahedra. According to magnetic measurements $K_2NaOsO_{5.5}$ is diamagnetic, whereas $K_3NaOs_2O_9$ displays strong antiferromagnetic coupling ($T_N=140$ K), indicating enhanced magnetic interactions within the octahedral pair.

1. Introduction

A peculiar characteristic of the perovskite structure type is its ability to accommodate almost any metal of the periodic table. In its archetypical formula ABO_3, "*A*" commonly represents a larger, electropositive cation, while "*B*" is smaller and bears a higher charge. If charge or size combinations of cations are incompatible with the ideal perovskite structure, the structure has many options to flexibly respond by adopting lower symmetries [1,2] or by allowing for mixed or deficient atomic site occupancies [3,4]. Partial chemical substitution of the *B* cation may alter the basic formula ABO_3 sizeably to more complex compositions like $A_2BB'O_6$ and $A_3BB'_2O_9$. In the latter cases, ordered crystal structures, known as double and triple perovskites, respectively, result if the *B* and *B*′ cations differ sufficiently in size or charge. The crystal structures are built from close packed layers of the oxygen atoms and the larger *A* cations, resulting in a cubic close packing in case of the double perovskites, while in triple perovskites the layers are stacked in an *ABACBC* sequence. The smaller *B* cations are filling the respective octahedral voids formed by the anions only. Perovskite type oxides are being extensively studied owing to their interesting electronic and magnetic properties. The focus on exploring new oxides containing a platinum group metal, especially osmium, has attracted considerable interest after discovering superconductivity in KOs_2O_6, which is a defect pyrochlore [5].

While a large number of double perovskites accommodating a considerable diversity of metals are known, those containing alkali metals are relatively rare. In continuation of early works on double perovskites with osmium and an alkali metal at the *B* site by Sleight et al. [6], recently a number of perovskite type oxides containing alkali metal atoms has been discovered within the group of platinum metals, particularly by zur Loye and co-workers [7–16]. Among the examples found there are mixed valent ruthenium(V/VI) [7], iridium(V/VI) [8,9], and mixed iridium-ruthenium containing triple perovskites [10] featuring interesting magnetic interactions. Also double perovskite osmates with strontium, barium or a lanthanide element at the *A* site have been reported [11–15]. However, only one triple perovskite containing osmium has been explored to date containing divalent barium as the *A* cation along with sodium as a *B* cation [16]. In general, also triple perovskites containing an alkali metal at the *A* site are still very rare. $K_3NaRe_2O_9$ [17] was reported more than a decade ago in this category. For the synthesis of the perovskites mentioned above, various methods have been applied, e.g., traditional solid state approaches by heating respective carbonates or nitrates, hydroxide flux methods, and high pressure routes reacting oxides and/or peroxides. Another technique, which has been applied in this work, is to react the alkali metal oxides under oxygen pressure [18]. This approach provides access to high oxidation states of the platinum metals, e.g., ruthenium has been oxidized to a pentavalent [19,20] or hexavalent state [21–23], while osmium has been realized with oxidation numbers seven [24,25] or even eight [26,27]. We regard the perovskite type of

---

* Corresponding author. Fax: +49 711 6891502.
E-mail address: M.Jansen@fkf.mpg.de (M. Jansen).

[1] Present address: Department of Chemistry and Biochemistry, Universität Bern, Freiestrasse 3, 3012 Bern, Switzerland.

[2] Present address: Department Chemie, Technische Universität München, Lichtenbergstraße 4, 85747 Garching, Germany.

0022-4596/$ - see front matter © 2012 Elsevier Inc. All rights reserved.
http://dx.doi.org/10.1016/j.jssc.2012.03.012

structure ideally suited to accommodate osmium in high oxidation states. To realize high oxidation states of the *B*-cation in any variant of the perovskite structure family, one needs to substitute the commonly used di- or tri-valent *A* site cations by (sufficiently large) monovalent cations. Respective attempts have resulted in the first osmium containing double and triple perovskites with alkali metal cations at both the *A* and *B* sites.

2. Experimental

For the preparation of $K_2NaOsO_{5.5}$, stoichiometric amounts of potassium superoxide (KO_2, Aldrich), sodium peroxide (Na_2O_2, Aldrich) and osmium powder (Chempur, 99.9%) were mixed in the ratio of 2:0.5:1, finely ground in an agate mortar, and pressed into pellets in argon atmosphere. The pellets were put into gold crucibles, which were sealed from one side and mechanically closed from the other. All these manipulations were performed in a glove box (MT 200, MBraun; $H_2O/O_2 < 0.01$ ppm). The crucibles were further placed into a stainless steel autoclave and allowed to react under oxygen pressure [18]. Black crystalline samples were obtained under an oxygen pressure of 35 MPa at a temperature of 673 K within 2 days, using sodium hydroxide as a mineralizer. Alternatively, single phase powder samples of $K_2NaOsO_{5.5}$ can be obtained from KO_2, Na_2O_2, and osmium powder under oxygen flow at 698 K. However, working in a closed system is favourable because to the formation of toxic and volatile OsO_4.

Initially, $K_3NaOs_2O_9$ was obtained as a by-product of the syntheses of $K_2NaOsO_{5.5}$. Pure samples are accessible by reaction of potassium superoxide (KO_2, Aldrich), sodium peroxide (Na_2O_2, Aldrich) and osmium powder (Chempur, 99.9%) in the ratio 2:1:2. All manipulations were carried out as described above for $K_2NaOsO_{5.5}$. Black crystalline samples were obtained in stainless steel autoclaves at a temperature of 873 K and an oxygen pressure of 35 MPa in 2 days. Both the products are hygroscopic and readily release osmium tetroxide upon exposure to air. Single crystals suitable for X-ray diffraction studies were selected in a glove box and sealed into glass capillaries of 0.3 mm diameter.

Single crystal X-ray data of both compounds were collected on a Bruker AXS with SMART-CCD (APEX) (MoK_α Graphite monochromator, semi-empirical absorption correction with the programme SADABS [28]). The crystal structure was solved and refined using the programme package SHELXTL [29]. Further information concerning the data collection and processing, the crystallographic parameters, as well as details on structure solution and refinement are given in Table 1. Details of the crystal structure investigation are available from the Fachinformationszentrum Karlsruhe, D-76344 Eggenstein-Leopoldshafen (Germany), on quoting the depository numbers CSD-423653 ($K_2NaOsO_{5.5}$) and CSD-423654 ($K_3NaOs_2O_9$).

Magnetic measurements were performed on a SQUID-Magnetometer (MPMS 5.5, Quantum Design) between 5 K and 350 K in magnetic fields up to 5 T.

Measurements of the electrical conductivity were performed on $K_2NaOsO_{5.5}$ and $K_3NaOs_2O_9$ by the four-point-probe method (Van-der-Pauw) on pressed pellets (diameter: 6 mm, thickness: 1 mm).

Raman spectra were recorded with a Confocal Microscope Laser Raman System (Jobin-Yvon, excitation line 632 nm, power 4 mW) for both compounds (Fig. 1(a) and (b)). Different modes were obtained, however, no relevant spectral data were found in the literature to assign all the modes except the mode at 859 cm^{-1} in $K_2NaOsO_{5.5}$ for OsO_6 octahedra [30]. The Raman modes monitored for $K_2NaOsO_{5.5}$ are: 288 cm^{-1}, 337 cm^{-1}, 382 cm^{-1}, 462 cm^{-1}, 563 cm^{-1}, 643 cm^{-1}, 699 cm^{-1}, 777 cm^{-1}, 821 cm^{-1}, 859 cm^{-1}; for $K_3NaOs_2O_9$: 223 cm^{-1}, 346 cm^{-1}, 416 cm^{-1}, 642 cm^{-1}, 738 cm^{-1}, 846 cm^{-1}.

Thermal analyses were carried out by using a DTA/TGA equipment (STA 409, Netzsch, Selb) coupled with a quadruple mass spectrometer. The samples were heated at the rate of 10 K min^{-1} in a corundum crucible under a flow of dry argon (Tables 2–4).

3. Results and discussion

According to a single crystal structure analysis, $K_2NaOsO_{5.5}$ crystallizes as double perovskite. The undistorted cubic structure with space group $Fm\bar{3}m$ is in accordance with the Goldschmidt tolerance factor [1] of 0.99, as calculated from the ionic radii of the constituents [31]. Na and Os are in perfectly octahedral coordination, with Na–O and Os–O distances of 2.347(4) Å and 1.862(4) Å, respectively. The potassium atom is surrounded by a

Table 1
Crystallographic data and details of the structure determinations for K_2NaOsO_6 and $K_3NaOs_2O_9$.

	$K_2NaOsO_{5.5}$	$K_3NaOs_2O_9$
Space group	$Fm\bar{3}m$ (No. 225)	$P6_3/mmc$ (No. 194)
Lattice parameters at 293 K	a=8.4184(5) Å	a=5.9998(4) Å, c=14.3053(14) Å
Cell volume	596.61(6) $Å^3$	445.97(6) $Å^3$
Formula units	4	2
Molar mass	387.39 g mol^{-1}	664.69 g mol^{-1}
X-ray density	4.313 g cm^{-3}	4.950 g cm^{-3}
Wavelength	Mo K_α	Mo K_α
Absorption coefficient	22.803 mm^{-1}	29.939 mm^{-1}
Temperature	293(2) K	293(2) K
2θ-region	$8.38^\circ < 2\theta < 69.86^\circ$	$5.70^\circ < 2\theta < 59.90^\circ$
hkl_{min}–hkl_{max}	$-13 \le h \le 13$, $-13 \le k \le 13$, $-13 \le l \le 13$	$-8 \le h \le 8$, $-8 \le k \le 8$, $-20 \le l \le 20$
Measured reflections	2381	5187
Unique reflections	96	290
R_{int}	0.0353	0.0426
Absorption correction	semi-empirical	semi-empirical
Reflections $> 2\sigma$	96	278
Number of parameters	8	22
$R(F)$(obs), $R(F)$(all)	1.40%, 1.40%	2.85%, 3.04%
$R_w(F^2)$(obs), $R_w(F^2)$(all)	4.00%, 4.00%	5.36%, 5.42%
Extinction coefficient	0.0034(4)	0.0013(3)
Difference density min./max.	−0.84/0.68 e $Å^{-3}$	−2.28/1.53 e $Å^{-3}$
Depository no.	CSD-423653	CSD-423654

cuboctahedron of O atoms, which is slightly distorted due to the different sizes of the NaO_6 and OsO_6 octahedra, resulting in rectangles instead of squares and equilateral triangles of two different sizes as faces.

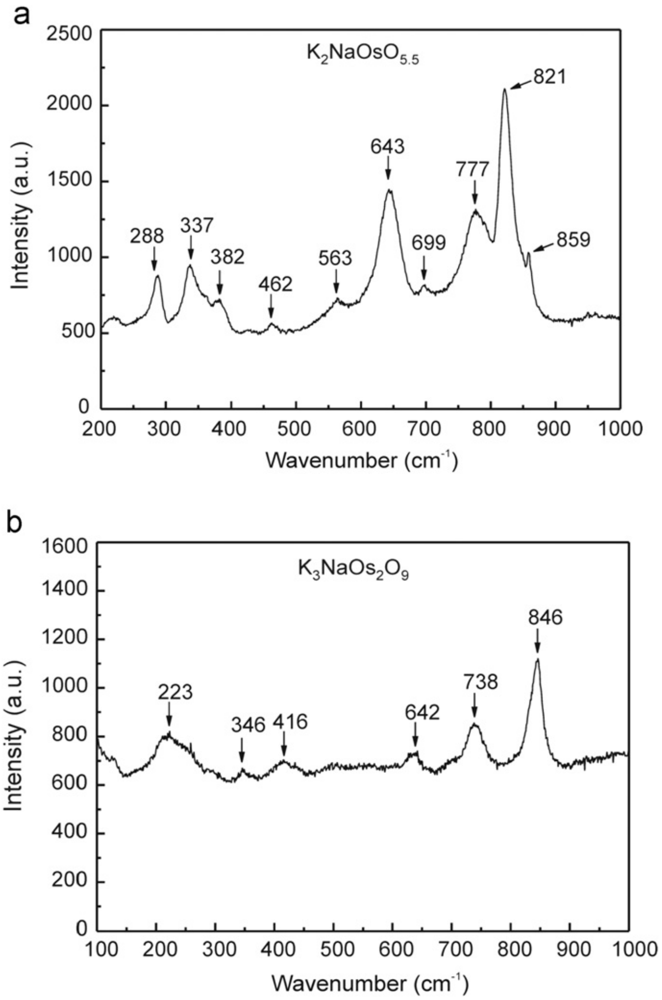

Fig. 1. Raman spectra of $K_2NaOsO_{5.5}$ (a) and of $K_3NaOs_2O_9$ (b).

Full occupation of all cationic and anionic sites would result in unbalanced sums of positive and negative charges. There are three options to establish charge neutrality, (1) underoccupation of the oxygen sites by a factor of 11/12, (2) mixed Na/Os occupation of the sodium *B* site and (3) partial replacement of oxide by hydroxide. We exclude possibility (3) because $K_2NaOsO_{5.5}$ can be prepared along a completely anhydrous route and because of any pertinent signature in the IR-spectra lacking, which is a very sensitive probe for the presence or absence of OH. The structure determination presented is of high precision. Refinement of a mixed occupation of the sodium site by 1/7 Os and 6/7 Na, as required for electroneutrality, resulted in physically meaningless large atomic displacement parameters (fixed s.o.f.'s) or in zero occupation for Os (variable s.o.f.'s). We thus also rule out option (2). It is obviously hard to positively verify possibility (1), because oxygen is a weakly scattering atom in the crystal under consideration, and trying to corroborate a site occupation of 11/12 by least squares refinements will not yield conclusive results, also because of strong correlations between s.o.f.'s and atomic displacement factors. The result we obtained indicated an occupation slightly above 1, without any effect on the *R* values and residual electron densities. For all the above mentioned reasons, we assume a composition $K_2NaOsO_{5.5}$ with fully occupied cation sites and a statistical disorder of vacancies of the oxygen sites.

The oxidation state +8 for osmium in $K_2NaOsO_{5.5}$ is confirmed by the diamagnetism as obtained from susceptibility measurements. Similar diamagnetic behaviour has been found in other osmium(VIII) oxides, K_2OsO_5 [26] and $Ag_{13}OsO_6$ [27], which had been synthesized under oxygen pressure using the same autoclave technique.

Analogously to these two Os(VIII) compounds, $K_2NaOsO_{5.5}$ is black. Considering the colour of the binary oxides K_2O, Na_2O (both colourless), and OsO_4 (pale yellow), the dark colour of the new double perovskite as well as of K_2OsO_5, which are both insulators ($Ag_{13}OsO_6$ is a metallic conductor), is not to be expected. The dark colours of these two oxides are presumably caused by charge transfer processes between the oxygen atoms and the highly charged osmium atoms.

In contrast, $K_3NaOs_2O_9$ contains osmium in a heptavalent state and crystallizes in the hexagonal 6H-$BaTiO_3$ type of structure, also known as triple perovskite. In terms of packing, a triple perovskite is a combination of cubic and hexagonal stacked layers of oxygen and potassium atoms with an *ABACBC* layer sequence. The resulting

Table 2
Atomic coordinates and displacement parameters [Å^2] for $K_2NaOsO_{5.5}$ and $K_3NaOs_2O_9$.

$K_2NaOsO_{5.5}$					
Atom	Wyckoff-Pos.	*x*	*y*	*z*	U_{11}
K	8*c*	1/4	1/4	1/4	0.0360(5)[a]
Na	4*b*	1/2	0	0	0.0293(12)[a]
Os	4*a*	0	0	0	0.0276(2)[a]
O	24*e*	0.2212(5)	0	0	0.0215(19), U_{22}=0.0300(13)[b]
$K_3NaOs_2O_9$					
Atom	Wyckoff-Pos.	*x*	*y*	*z*	U_{iso}
K(1)	2*b*	0	0	1/4	0.0225(10)
K(2)	4*f*	1/3	2/3	0.1100(3)	0.0274(8)
Na	2*a*	0	0	0	0.0158(17)
Os	4*f*	2/3	1/3	0.14948(4)	0.0139(2)
O(1)	6*h*	0.5305(8)	0.0610(16)	1/4	0.0175(18)
O(2)	12*k*	0.3667(13)	0.1834(7)	0.0916(5)	0.0279(15)

[a] $U_{11}=U_{22}=U_{33}=U_{iso}$, $U_{23}=U_{13}=U_{12}=0$.
[b] $U_{22}=U_{33}$, $U_{23}=U_{13}=U_{12}=0$.

Table 3
Anisotropic displacement parameters [Å^2] for $K_3NaOs_2O_9$.

$K_3NaOs_2O_9$						
Atom	U_{11}	U_{22}	U_{33}	U_{23}	U_{13}	U_{12}
K(1)	0.0241(15)	0.0241(15)	0.019(2)	0	0	0.0121(7)
K(2)	0.0233(10)	0.0233(10)	0.0356(19)	0	0	0.0117(5)
Na	0.018(2)	0.018(2)	0.012(4)	0	0	0.0089(12)
Os	0.0147(2)	0.0147(2)	0.0123(3)	0	0	0.00733(11)
O(1)	0.018(3)	0.010(4)	0.022(4)	0	0	0.005(2)
O(2)	0.015(3)	0.034(3)	0.028(3)	−0.0055(15)	−0.011(3)	0.0075(16)

Table 4
Selected bond lengths [Å] and angles in $K_2NaOsO_{5.5}$ and $K_3NaOs_2O_9$.

$K_2NaOsO_{5.5}$			
Atoms	Distances	Atoms	Distances
K–O	2.9862(4) [12 ×]	Os–O	1.862(4) [6 ×]
Na–O	2.347(4) [6 ×]		
$K_3NaOs_2O_9$			
Atoms	Distances	Atoms	Angles
K1–O1	3.0166(9) [6 ×]	O1–Os–O2	162.5(3)° [3 ×]
K1–O2	2.960(7) [6 ×]	O1–Os–O1	74.8(3)° [3 ×]
K2–O1	2.865(7) [3 ×]	O1–Os–O2	91.4(2)° [6 ×]
K2–O2	3.0164(9) [6 ×]	O2–Os–O2	99.8(3)° [3 ×]
K2–O2	3.279(8) [3 ×]	Os–O1–Os	90.9(3)° [3 ×]
Na–O1	2.313(6) [6 ×]		
Os–O1	2.017(6) [3 ×]		
Os–O2	1.764(7) [3 ×]		
Os–Os	2.8760(11)		

octahedral voids are linked in part pairwise face sharing and by common vertices, as shown in Fig. 2. All pairs of face sharing octahedra are occupied by osmium, while the single octahedra are filled by sodium.

The potassium atoms are twelvefold coordinated by cuboctahedra and anticuboctahedra of oxygen atoms. The K–O and Na–O distances are in good agreement with those observed in the rhenium analogue, $K_3NaRe_2O_9$ [17]. Within the Os_2O_9 octahedra pair the osmium atoms are displaced by 0.21 Å from the octahedron centre and therefore two considerably different Os–O distances are observed. The long Os–O distances of 2.017(6) Å are formed by the set of three oxygen atoms that constitute the shared face of the octahedra pair, while the short distances of 1.764(7) Å are those to the outer set of six oxygen atoms connecting to the NaO_6 octahedra. The Os–O distance measuring ~2 Å is typical for this set of M–O separations in triple perovskites. The heavy off-centring of the Os atoms is obviously caused by the strong coulomb repulsion of the highly charged cations. Accordingly, the Os–Os interatomic distance of 2.876(1) Å is larger than those in $Ba_3NaOs_2O_9$ (2.549 Å) [16] with Os in a formal oxidation state of +5.5 and in osmium metal (2.675 Å), but even shorter than in the rhenium analogue (Re–Re 2.92 Å) [17].

It has to be noted, that a ruthenate with the corresponding cation composition K/Na/TM 3:1:2, which has been obtained at similar reaction conditions, $K_3NaRu_2O_8$ [23], contains Ru(VI) and crystallises in the Glaserite type of structure with tetrahedral $(RuO_4)^{2-}$ anions.

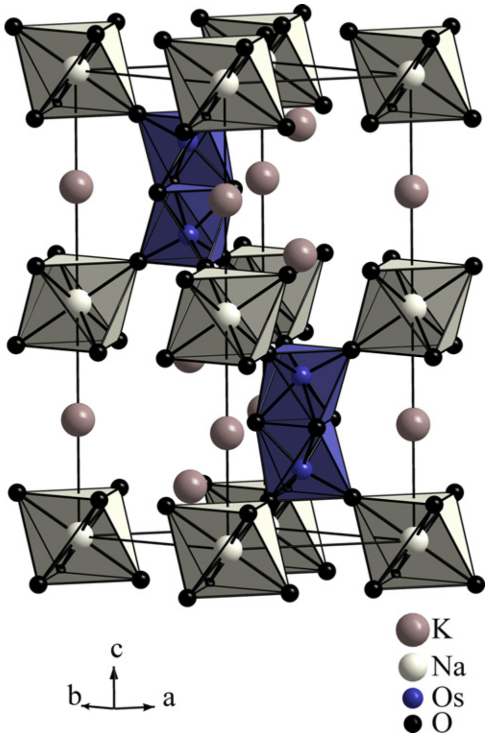

Fig. 2. Crystal structure of $K_3NaOs_2O_9$, Os_2O_9 groups are drawn as dark, NaO_6 octahedra as light polyhedra.

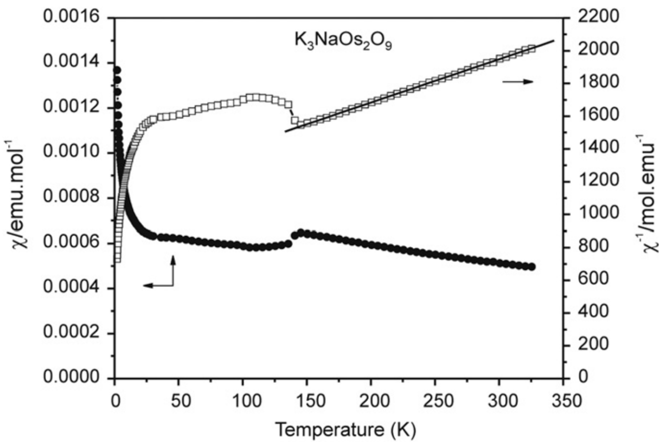

Fig. 3. Susceptibility and inverse susceptibility against temperature in an applied field of 1 T. The solid line on the inverse susceptibility curve represents a linear fit for calculating the magnetic moment.

The short Os–Os and Os–O distances give rise to strong magnetic interactions. $K_3NaOs_2O_9$ displays paramagnetic behaviour and undergoes a magnetic transition at around 140 K. Susceptibility curves measured in an applied field of 1 T are shown in Fig. 3. The inverse magnetic susceptibility obeys the Curie–Weiss law down to about $T=150$ K. Further, after a slight increase at 140 K, the inverse susceptibility drops to zero with decreasing temperature. Above 150 K, an effective magnetic moment of

$\mu_{eff}=0.87\ \mu_B$ can be extracted with a tentatively applied Curie–Weiss law fit from 150 K to 320 K. The large negative characteristic Curie–Weiss temperature $\Theta=-436$ K is indicative for frustrated magnetic interactions. A strongly reduced effective moment, in case of $K_3NaOs_2O_9$ equivalent of less than 0.5 unpaired electrons per osmium, was also found for iridium in $Ba_3BiIr_2O_9$ [32] and seems to be typical for M_2O_9 structural dimers due to strong hybridization effects [33,34]. To reveal the magnetic coupling and the structural or magnetic nature of the transition at 140 K, further neutron and low temperature studies are required.

Both the compounds are insulating in the investigated temperature range of 1.5 K to 350 K. At around 473 K, both compounds start evolving oxygen continuously up to 1273 K. From $K_2NaOsO_{5.5}$ an intermediate of the nominal composition "K_2NaOsO_5", based on weight loss calculations, forms at 773 K.

Acknowledgements

The authors thank Dr. J. Nuss for recording the single crystal data, E. Bruecher for SQUID measurements, G. Siegle for conductivity measurements, A. Schulz for Raman measurements, and Dr. C. Oberndorfer for DTA measurements.

Appendix A. Supporting information

Supplementary data associated with this article can be found in the online version at http://dx.doi.org/10.1016/j.jssc.2012.03.01.

References

[1] V.M. Goldschmidt, Naturwissenschaften 14 (1926) 477–485.
[2] P.M. Woodward, Acta Crystallogr. B 53 (1997) 44–66.
[3] F. Galasso, L. Katz, R. Ward, J. Am. Chem. Soc. 81 (1959) 820–823.
[4] H. Samata, M. Kai, T. Uchida, M. Ohtsuka, G. Tanaka, S. Sawada, T. Taniguchi, Y. Nagata, J. Alloys Compd. 350 (2003) 77–85.
[5] S. Yonezawa, Y. Muraoka, Y. Matsushita, Z. Hiroi, J. Phys. Condens. Matter 16 (2004) L9–L12.
[6] A.W. Sleight, J. Longo, R. Ward, Inorg. Chem. 1 (1962) 245–250.
[7] K.E. Stitzer, M.D. Smith, W.R. Gemmill, H.-C. zur Loye, J. Am. Chem. Soc. 124 (2002) 13877–13885.
[8] S.J. Kim, M.D. Smith, J. Darriet, H.-C. zur Loye, J. Solid State Chem. 177 (2004) 1493–1500.
[9] H.-C. zur Loye, R.B. Macquart, S.-J. Kim, M.D. Smith, Y. Lee, T. Vogt, Solid State Sci. 11 (2009) 608–613.
[10] M. Lufaso, H.-C. zur Loye, Inorg. Chem. 44 (2005) 9154–9161.
[11] C. Tian, A.C. Wibowo, H.-C. zur Loye, M.-H. Whangbo, Inorg. Chem. 50 (2011) 4142–4148.
[12] K.E. Stitzer, M.D. Smith, H.-C. zur Loye, Solid State Sci. 4 (2002) 311–316.
[13] W.R. Gemmill, M.D. Smith, R. Prozorov, H.-C. zur Loye, Inorg. Chem. 44 (2005) 2639–2646.
[14] M.D. Smith, W.R. Gemmill, H.-C. zur Loye, J. Solid State Chem. 179 (2006) 1750–1756.
[15] S.J. Mugavero III, W.R. Gemmill, I.P. Roof, H.-C. zur Loye, J. Solid State Chem. 182 (2009) 1950–1963.
[16] K.E. Stitzer, A.E. Abed, M.D. Smith, M.J. Davis, S.J. Kim, J. Darriet, H.-C. zur Loye, Inorg. Chem. 42 (2003) 947–949.
[17] K.-J. Range, A. Atzesdorfer, Z. Naturforsch. 48b (1993) 237.
[18] C. Linke, M. Jansen, Z. Anorg. Allg. Chem. 623 (1997) 1441–1446.
[19] W. Klein, M. Jansen, Acta Crystallogr. C 61 (2005) i1–i2.
[20] W. Klein, R.K. Kremer, M. Jansen, J. Mater. Chem. 17 (2007) 1356–1360.
[21] K.M. Mogare, K. Friese, W. Klein, M. Jansen, Z. Anorg. Allg. Chem. 630 (2004) 547–552.
[22] D. Fischer, R. Hoppe, K.M. Mogare, M. Jansen, Z. Naturforsch. 60b (2005) 1113–1117.
[23] K.M. Mogare, W. Klein, E.-M. Peters, M. Jansen, Solid State Sci. 8 (2006) 500–507.
[24] K.M. Mogare, W. Klein, H. Schilder, H. Lueken, M. Jansen, Z. Anorg. Allg. Chem. 632 (2006) 2389–2394.
[25] K.M. Mogare, W. Klein, M. Jansen, Acta Crystallogr. E. 62 (2006) i52–i54.
[26] K.M. Mogare, W. Klein, M. Jansen, Z. Anorg. Allg. Chem. 631 (2005) 468–471.
[27] S. Ahlert, W. Klein, O. Jepsen, O. Gunnarsson, O.K. Andersen, M. Jansen, Angew. Chem. 115 (2003) 4458–4461. Angew. Chem. Int. Ed. 42 (2003) 4322–4325.
[28] G.M. Sheldrick, Bruker AXS Inc., SADABS, Madison, Wisconsin, USA, 1998.
[29] G.M. Sheldrick, Acta Crystallogr. A 64 (2008) 112–122.
[30] J. Weidlein, U. Müller, K. Dehnicke, Schwingungsfrequenzen II: Nebengruppenelemente, Georg Thieme Verlag, Stuttgart, New York, 1986.
[31] R.D. Shannon, Acta Crystallogr. A 32 (1976) 751–767.
[32] W. Müller, M. Avdeev, Q. Zhou, B.J. Kennedy, N. Sharma, R. Kutteh, G.J. Kearley, S. Schmid, K.S. Knight, P.E.R. Blanchard, C.D. Ling, J. Am. Chem. Soc. 134 (2012) 3265–3270.
[33] Y. Doi, Y. Hinatsu, J. Phys. Condens. Matter 16 (2004) 2849–2860.
[34] J.-G. Cheng, J.-S. Zhou, J.A. Alonso, J.B. Goodenough, Y. Sui, K. Matsubayashi, Y. Uwatoko, Phys. Rev. B 80 (2009) 104430-1–104430-9.